ZIBELINE INTERNATIONAL™ PUBLISHING

ISSN: 2633-4062 (Print)
ISSN: 2633-4070 (Online)
CODEN: ECCCB9

Ecofeminism and Climate Change (EFCC)

DOI: http://doi.org/10.26480/efcc.01.2026.17.29

RESEARCH ARTICLE

IMPACT OF CLIMATE CHANGE AND LAND USE/LAND COVER CHANGES ON SUSTAINED WATER FLOW IN THE TAMNE CATCHMENT OF GHANA: A LONG-TERM SPATIO-TEMPORAL ASSESSMENT USING THE SWAT MODEL

Robert Asaanbilla Awini[a], Steve Ampofo[b], Melvin Guy Adonadaga[b], Boateng Ampadu[b]

[a] Department of Science, Garu Commmunity Day Senior High School, Box 2, Upper East Region, Ghana.
[b] Department of Environmental Science, School of Environment and Life Sciences, C.K. Tedam University of Technology and Applied Science (UTAS), Navrongo, Ghana.
**Corresponding Author Email: robertasaanbill@gmail.com*

ARTICLE DETAILS

Article History:

Received 20 January 2026
Revised 26 January 2026
Accepted 12 February 2026
Available online 19 February 2026

ABSTRACT

Tamne catchment has a river system, a reservoir, and fertile arable land, making it a valuable landscape in the northern part of Ghana. Tamne catchment's water flow is crucial, and long-term spatio-temporal assessment from 1992 to 2022 to understand inter-decadal variability is essential for supporting water management and agriculture in the catchment. The study used geospatial and climate data and applied the SWAT model and Mann-Kendall test with Sen's slope to assess key climatic and LULC variables. The results showed that water increased by 1%, built/bare soil areas increased by 26% while grass/shrub land decreased by 31% from 1992-2022, and agricultural land saw a decline by 37% and 28% between 2002 and 2022. Climate and LULC shifts increased evapotranspiration and led to decreasing trends in groundwater and surface discharge. Trend analysis of rainfall indicated a troubling decline in rainfall with a Sen's slope of -5.24, highlighting variability in the annual rainfall but insignificantly affects the catchment hydrology. The SWAT model performed well, supported with an NSE of 0.71 and robust P- and R-factor values of 0.75 and 0.78, respectively.

KEYWORDS

Climate, Variability, Landuse, Landcover, Hydrology, Tamne.

1. INTRODUCTION

The Tamne Catchment in Ghana's Upper East Region plays a vital role in supporting the livelihoods of local communities, serving as a critical source of water for agriculture, domestic use, and sustaining natural ecosystems. Additionally, Tamne River and reservoir (dam) are both serving as natural and artificial sinks created to hold water for conservation of aquatic natural habitats and its valley for lowland agricultural production and other economic uses. However, this catchment is increasingly under pressure from a combination of land use and land cover changes, driven by population growth, agricultural expansion, and urbanization (Obuobie, et al., 2012). These anthropogenic activities have significantly altered the natural landscape, leading to the degradation of vegetation, and changes in the hydrological cycle (Issahaku, 2023; Nasta, et al., 2020; Trenberth, 2011).

The interplay between land use, land cover, and climate change has become a focal point in understanding environmental transformations, particularly in regions where livelihoods are closely tied to natural resources (IPCC, 2022; Issahaku, 2023). The Tamne Catchment, located in Ghana's Upper East Region, is an area where these interactions are especially pronounced (Okofo, and Martienssen, 2022). As a semi-arid region, the catchment is already vulnerable to climatic fluctuations (Ampadu, et al., 2019; Ampofo, et al., 2023; Asante, and Amuakwa-Mensah, 2014), and the pressures from human activities are compounding the situation. Over recent decades, the Tamne Catchment has experienced significant changes in land use and land cover, driven by agricultural expansion, urbanization, and other socio-economic developments (Mishio, 2021). These changes, in conjunction with the impacts of climate change such as altered precipitation patterns and increasing temperatures, are reshaping the catchment's landscape and its hydrological processes (Asamoah, and Ansah-Mensah, 2020; Copernicus, 2023; Klutse, et al., 2020; Maru, et al., 2023).

This study explores the cumulative impacts of these changes on the Tamne Catchment, focusing on how shifts in land use and land cover, coupled with climate variability, are affecting water resources (Abbas, et al., 2022; Awotwi, et al., 2019; Kpoti, et al., 2016). By analyzing remote sensing data, hydrological models, and local observations through ground truthing, this research aims to unravel the complex interactions between human activities and natural processes (Awotwi, et al., 2021; Baker, and Miller, 2013). The study therefore specifically examined the impacts of changes in land use and land cover on the Tamne Catchment, analyzed rainfall patterns focusing on temporal distribution and variability over a 30-year time series, and carried out a hydrologic parametric sensitivity analysis using the Soil and Water Assessment Tool (SWAT).

Understanding these dynamics is crucial for developing sustainable land and water management strategies that can mitigate the adverse effects of these changes and enhance the resilience of the Tamne Catchment in the face of ongoing environmental challenges.

2. MATERIALS AND METHODS

2.1 Description of the Tamne Catchment

The Tamne catchment is largely drained by the Tamne River, situated in the Upper East Region within the White Volta basin. It spans across the Garu and Tempane districts, sharing boundaries with the Bawku Municipality and Binduri districts, situated in the Northern Savanna Agro-

Quick Response Code	Access this article online	
	Website: www.efcc.com.my	DOI: 10.26480/efcc.01.2026.17.29

Cite The Article: Robert Asaanbilla Awini, Steve Ampofo, Melvin Guy Adonadaga, Boateng Ampadu (2026). Impact of Climate Change and Land Use/Land Cover Changes on Sustained Water Flow in The Tamne Catchment of Ghana: A Long-Term Spatio-Temporal Assessment Using The Swat Model. Ecofeminism and Climate Change, 7(1): 17-29.

Climatic Zone of Ghana, as shown in (Figure 1). The Tamne reservoir, an important feature of the catchment, is estimated to hold approximately 179,036,094.26 m^3 of surface water (Ghana Irrigation Development Authority, 2021). Initially, the dam was designed to irrigate 1,500 hectares (equivalent to 3,706.58 acres) of land, but the current operational area under irrigation spans 799.98 hectares (1,976.8 acres), as reported by the Ghana Irrigation Development Authority (2021).

Covering a land area of 880 km^2, the Tamne sub-catchment accounts for 71.54% of the total land area of 1,230 km^2, extending across the Garu and Tempane districts (Ministry of Food and Agriculture, 2022). Geographically, it lies between latitudes 10°50'N and 11°18'N, and longitudes 0°08'W and 0°30'W. According to demographic data from the Ghana Statistical Service (2021), the population of the study area is estimated to be 158,767. With an altitude ranging between 120 m and 150 m above sea level (Asserup, and Eklöf, 2000; Okofo, and Martienssen, 2022), the Tamne catchment is susceptible to flooding during the rainy season, highlighting the seasonal hydrological dynamics and challenges faced by the local communities (Asserup, and Eklöf, 2000).

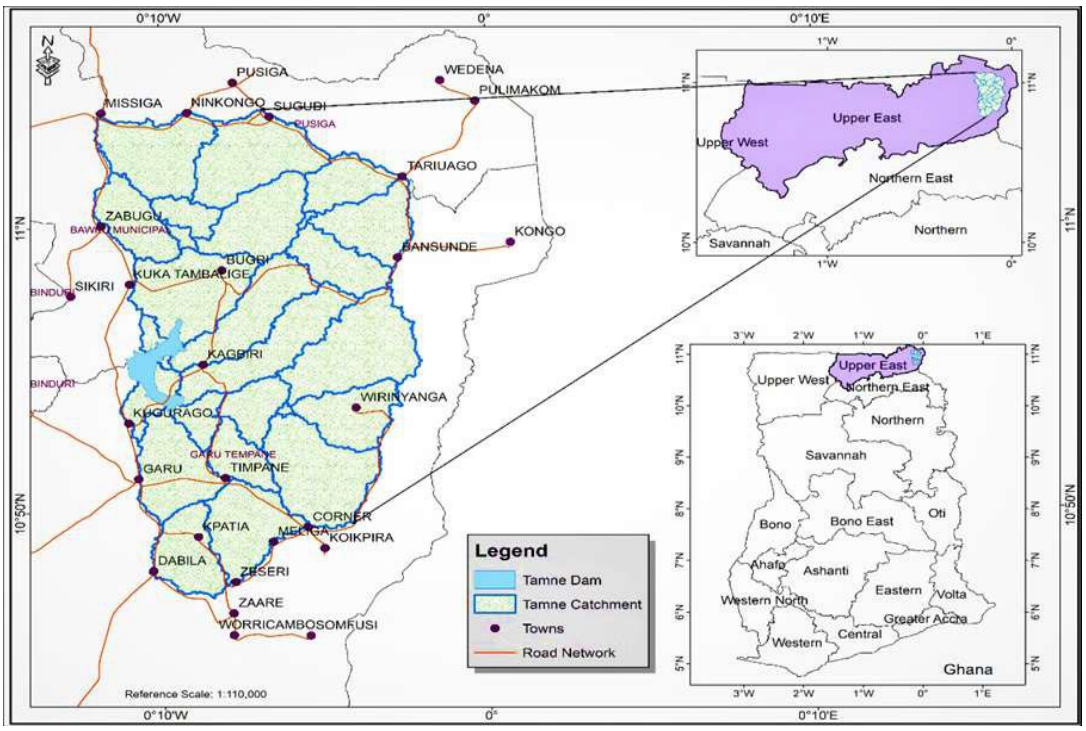

Figure 1: A map of Ghana showing the location of Tamne catchment and the river network

2.2 The SWAT model and its application

The Soil and Water Assessment Tool (SWAT®) is basically a process-based, semi-distributed hydrological model developed by the USDA Agricultural Research Service (Gassman, et al., 2014). It operates on a daily time step and is spatially explicit, representing hydrological response units (HRUs) within a river basin (Efthimiou, 2018). SWAT® uses inputs such as daily rainfall, air temperature, solar radiation, humidity, and wind speed to simulate hydrological processes (Gassman, et al., 2014). The model divides the catchment into sub-catchments, further segmented into HRUs (Guug, et al., 2020), characterized by homogeneous land use, vegetation, and soil characteristics (Gassman, et al., 2014). SWAT® simulates hydrological processes based on the water balance equation of a catchment (Awotwi, et al., 2019; Pandi, et al., 2023), considering factors such as precipitation, runoff, actual evapotranspiration, groundwater exchange, and change in storage (Dile, et al., 2016; Guug, et al., 2020).

The SWAT® model has been implemented through the ArcSWAT® interface, allowing for the prediction of environmental impacts of land use, management practices, and climate change (Kpoti, et al., 2016). Despite its complexity, SWAT® offers computational efficiency and long-term simulation capabilities, making it a valuable tool for assessing hydrological processes at catchment scales (Osei, et al., 2019). The efficiency of a model's predictions relies heavily on its setup and parameterization (Abbaspour, 2015; Xiang, et al., 2022). In the case of SWAT® modelling of water balance, this involves discretising the catchment and parameters into a spatially distributed format, selecting initial calibration parameter values, and configuring the time setup (IPCC, 2022). The catchment is divided into several sub-catchments using GIS software, with smaller sub-catchments representing topographically distinct regions such as rainfall or soil gradients (Guug, et al., 2020), along with the catchment's river network. The sub-catchment breakdown forms the node component of the catchment network used in the modelling process (Efthimiou, 2018).

SWAT® model requires various inputs, including digital elevation model, land use/land cover data, soil data, and climatic data, especially temperature and precipitation (Dile, et al., 2016; Guug, et al., 2020). These inputs are obtained from sources like the Food and Agriculture Organisation's Digital Soil Map of the World (FAO-DSMW©) and weather-observed data spanning a specified time period. Calibration of the model typically involves optimising parameters using observed data for a certain timeframe, followed by validation using separate observed data for verification (Abbaspour, 2015; Arnold, et al., 2012). For SWAT® modelling, the catchment is delineated into multiple sub-catchments and Hydrological Response Units (HRUs). The model setup includes assigning specific input data and configuring parameters such as DEM, soil type, land use, soil water content, and climate data (Baker, and Miller, 2013; Efthimiou, 2018). This setup allows for the simulation and analysis of hydrological processes within the catchment.

2.3 Data Sources and Analysis

Due to the lack of sufficient ground-point or station-gauged data within the Tamne catchment, coupled with the inherent errors present in the available climatic data, geospatial data derived from global atmospheric reanalysis and weather sources, as outlined in Table 1, were utilised as input variables. ArcGIS 10.3® with Landsat imagery and the ArcSWAT® extension were employed for digital elevation modelling, land use/land cover (LULC) mapping, soil classification, and hydrological measurements, as detailed in Figure 2, Figure 4, and Figure 5 respectively. Statistical analyses, including the Mann-Kendall test and Sen's slope estimator, were utilised to comprehensively understand the dynamics and trends of the land use/land cover as well as the hydro-climatic data, as demonstrated by (Sanogo et al., 2023; Wang et al., 2020).

The topographic data used for the digital elevation model and satellite imagery for land use and land cover (LULC) maps were both extracted from [USGS Earth Explorer] (https://earthexplorer.usgs.gov), while weather data was generated from [Global Weather - Texas A&M University] (https://globalweather.tamu.edu/). Soil grid data for soil mapping was obtained from FAO GeoNetwork (http://www.fao.org/geonetwork/srv/), which provides access to interactive maps as shown in (Figure 2), satellite imagery, and spatial databases (Efthimiou, 2018), maintained by the Food and Agriculture Organization (FAO).

Additionally, in-situ river discharge data sourced from the [Global Runoff Data Center (GRDC)] (https://www.bafg.de/GRDC/EN/Home/homepage_node.html) were used for model calibration and validation.

Cite The Article: Robert Asaanbilla Awini, Steve Ampofo, Melvin Guy Adonadaga, Boateng Ampadu (2026). Impact of Climate Change and Land Use/Land Cover Changes on Sustained Water Flow in The Tamne Catchment of Ghana: A Long-Term Spatio-Temporal Assessment Using The Swat Model. Ecofeminism and Climate Change, 7(1): 17-29.

Table 1: SWAT Input Datasets and Sources

Data type	Description	Resolution	Source
Digital Elevation Model (DEM)	Provides data and information on the slope and the river network of the catchment	30x30m	USGS Earth Explorer
Satellite Imagery for LULC Maps	Used for generating HRU in the HRU definition menu	30x30m	USGS Earth Explorer
Soil Map	Used in the generation of the HRU in the HRU definition menu	Scale: 1:5,000,000	FAO GeoNetwork
Weather Data	Daily Precipitation, maximum and minimum air temperature		Global Weather - Texas A&M University
Data of River Discharge	Discharge data used for standardisation and authentication of the model		Global Runoff Data Center (GRDC)

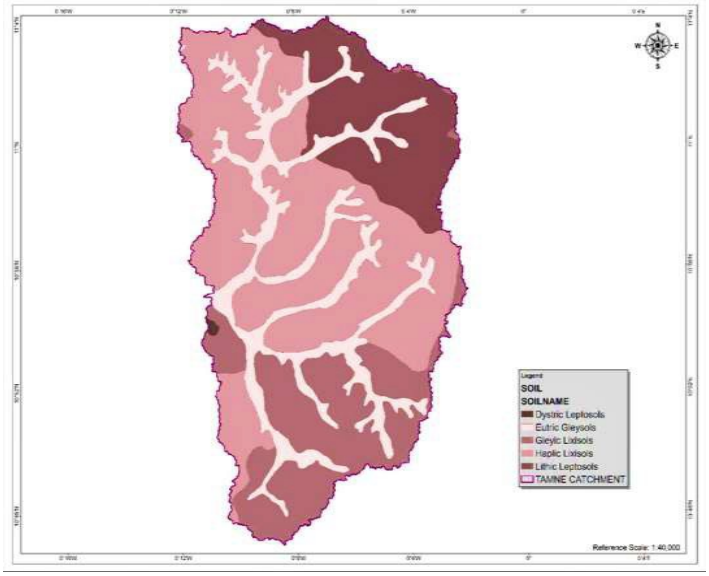

Figure 2: Soil map showing the classes of soil in the study area

2.4 Research Design Using Multi-Model Assessment under Climate Change

A multi-model-based assessment of spatial and temporal patterns of key climatic and hydrological variables across different time scales in the catchment is employed as part of the research design (Figure 3), and the modules are explained in Table 2. As validated by ground truthing in Table 3, Land use types delineation and classification using Landsat imagery in ArcGIS® 10.3 with ArcSWAT® extension was conducted to realise the consequences of changing patterns relative to land use or land cover (LULC) on the hydrology of the Tamne catchment (Khalid, 2018). This was validated by ground truthing data in (Table 2). Additionally, time series trend analysis incorporating the Mann-Kendall test with Sen's slope over 30 years from 1992 to 2022 was performed to assess water availability and water balance components using SWAT® model outputs from the ArcSWAT® interface (Dile et al., 2016). The analysis utilised ArcGIS® with ArcSWAT® extension to generate daily, monthly, or yearly time series of catchment-based climatic variables for climate- hydrological simulation, along with the XLSTAT interface for Mann-Kendall test and Sen's slope estimation.

Table 2: Ground Truthing Land use/land cover classes at a sample location with GPS Codes

LULC-Type	Location	GPS Code	GPS Coordinates	
			Latitude	Longitude
Water	Gagbri/Tamne	UG-4640-2729	10.9082	-0.1815
Built/Bare Soil Areas	Kugrago	UG-0030-5958	10.8677	-0.1770
Open Savannah Wood/Shrub land	Kugzua	UG-0363-4950	10.8642	-0.1337
Open Grassland with Shrubs	Nomboko	UG-0315-4968	10.8952	-0.2178
Agricultural land	Napaadi	UG-4554-0649	10.8986	-0.2089

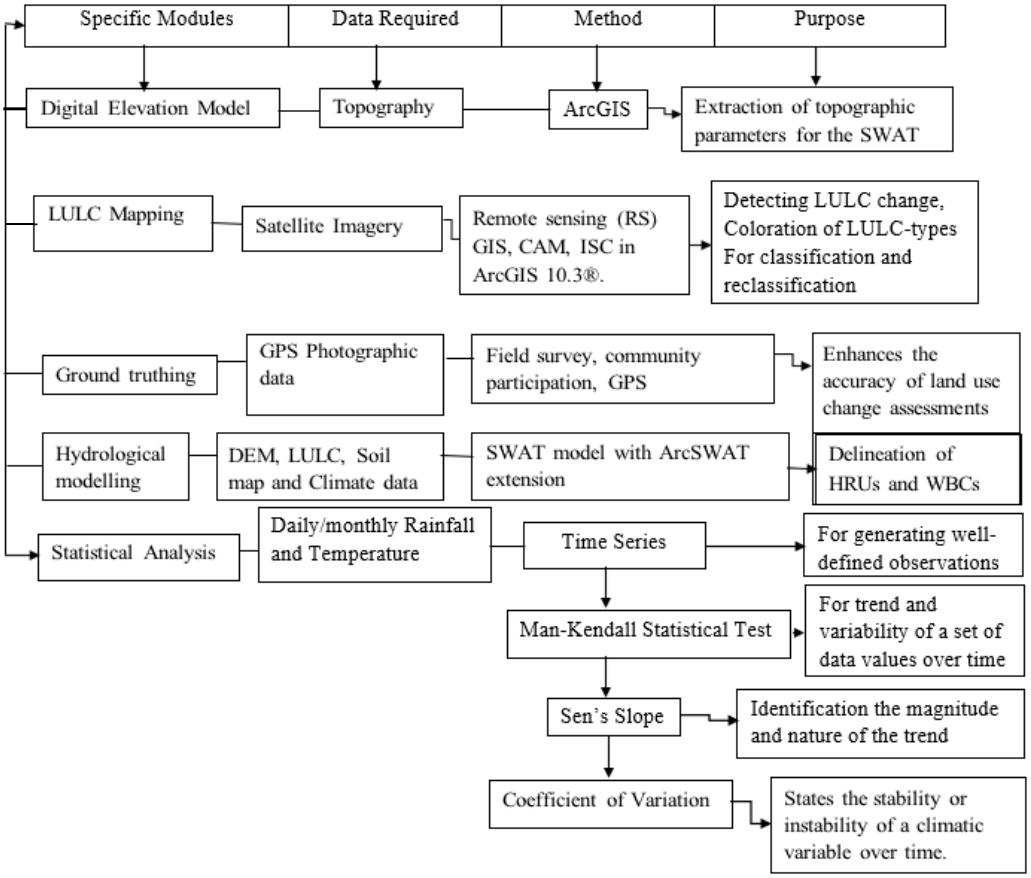

Figure 3: Multi-model assessment flow chart

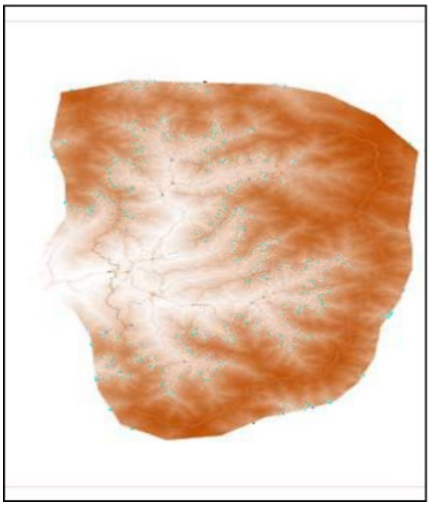

Figure 4: Digital Elevation Model

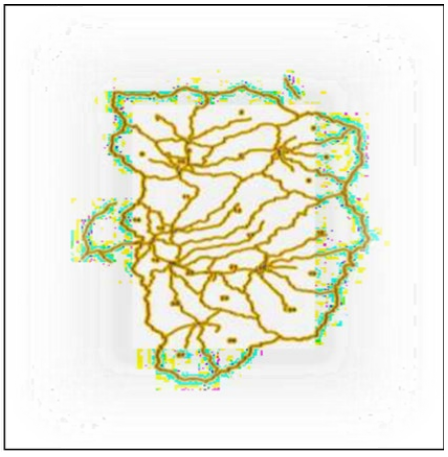

Figure 5: Delineation drainage of sub catchments

2.5 Statistical Analysis

Time series analysis was applied to generate well-defined observations over time and to identify trends at decadal and inter-decadal scales (Abbas et al., 2022; Quaye-Ballard et al., 2020).The Mann-Kendall test (MK-test) with Sen's slope was utilised to statistically assess the trend and variability in the data values over time, identifying the magnitude and nature of the trend (whether positive or negative). Also, a five-year moving average was estimated from the data to smooth the time series and measure the trend by removing the seasonal variation and adequately describing the general pattern of the time series.

2.5.1 Mann-Kendall statistical test

The Mann-Kendall (MK) statistical test, developed by Mann (1945) and Kendall (1975), is a rank-based non-parametric method used to detect trends in hydro-meteorological data such as precipitation and other water balance components (Sanogo et al., 2023; Yue et al., 2002). The Mann-Kendall test for trend can be performed in Excel using the XLSTAT® statistical software. It assesses whether a set of data values is increasing or decreasing over time and determines the statistical significance of any observed trend (Wang et al., 2020). The Mann-Kendall test statistic (S) indicates the direction of the trend (increasing or decreasing), while the variance Var(S) measures the dispersion of the data around the mean.

The Mann-Kendall test statistic (S) is computed as follows:

$$S = \sum_{i=1}^{n-1} \sum_{j=i+1}^{n} sgn\,(X_j - X_i) \quad (1)$$

$$Sgn\,(X_j - X_i) = \begin{cases} +1, if\ X_j - X_i > 0 \\ 0, if\ X_j - X_i = 0 \\ -1, if\ X_j - Xi < 0 \end{cases} \quad (2)$$

$$\mathrm{Var}(S) = n\,(n+1)\,(2n+5) - \sum_{i=1}^{m} t_i\,(t_1 - 1)\,(2t_1 + 5)\,/18. \quad (3)$$

2.5.2 Sen's slope Estimation

Sen's slope estimator is used to measure the magnitude of the trend in a series of data that is not serially autocorrelated. It estimates the gradient (or slope) of the trend in a sample of (S) two-array of data (Wang et al., 2020). The Sen's slope (Qi) is calculated using the formula:

$$Q_i = X_j - X_k / j - k \quad for\ i = 1\ldots., S. \quad (4)$$

Where:

(Xj) and (Xk) are the data values at times (j) and (k) (j > k), respectively.

2.5.3 Coefficient of variation

The coefficient of variation (CV) is a relative measure of dispersion used to determine the variability of a series of numbers regardless of the unit of measurement (Dagnachew et al., 2020; Osei et al., 2019). The coefficient of variation of large values indicates instability of the dependent variable,

while a small value means that the variable is stable (Abbaspour, 2015). CV is usually expressed in percentages. Coefficient of variation (CV) is given by:

$$CV = \sigma / \mu \quad (5)$$

Where:

CV is the coefficient of variation,

σ is the standard deviation, and

μ is the mean of the climatic time series data.

3. Results and Discussion

3.1 Land Use or Land Cover Change Mapping and Proportionality Analysis in the Catchment for 1992, 2002, 2012 and 2022

In Figure 6 and Table 3, with 1992 as the base year, indicates that, from 1992 to 2012, the water area (WAT) remained unchanged, covering 8.8 km^2 proportionally as 1%, but increased to17.6 km^2 representing 2% in 2022 after two consecutive decades. Built/bare soil areas (BBS) showed a proportional increase from 23% to 48% and 49% respectively, as shown in Table 4. The higher percentage change occurred between 2002 and 2012 by 25%, and only 1% increase between 2012 and 2022. The built and bare soil areas remained at 202.4 km^2 from 1992 to 2002 but increased to 422.4 km^2 and 431.2 km^2 in 2012 and 2022, representing 48% and 49%, respectively. Grass/shrub land (GLS) decreased proportionally from 50% in 1992 to 19% in 2022 (Figure 4). Proportionally, agricultural areas increased from 50% to 58% between 1992 and 2002. Agricultural land (AGR) use changed from 50% in 1992 to 58% in 2002 but decreased greatly to 21% and 30% in 2012 and 2022, respectively. The Land use/Land cover classification in Figure 6, have been validated by ground truthing data. In Figure 7. The inter-conversion matrix of land use/land cover and proportionality analysis is shown in Table 4.

Table 3: Proportionality of the area and percentage of LULC classes from 1992-2022

Period	1992		2002		2012		2022	
LULC type	Area (km^2)	%	Area (km^2)	%	Area (km^2)	%	Area (km^2)	%
Water	8.8	1	8.8	1	8.8	1	17.6	2
Built/Bare Soil-Areas	202.4	23	202.4	23	422.4	48	431.2	49
Grass/Shrub Land- Areas	228.8	26	158.4	18	264.0	30	167.2	19
Agricultural-Areas	440.0	50	510.4	58	184.8	21	264.0	30
Total	880.0	100	880.0	100	880.0	100	880.0	100

Table 4: Land Conversion and Proportionality Analysis

Period	From	To	Conversion (km2)	% Change
1992-2002	GSL	AGR	70.4	30.77
1992-2002	AGR	BBS	220.4	50.09
2002-2012	AGR	GSL	102.6	20.0

Cite The Article: Robert Asaanbilla Awini, Steve Ampofo, Melvin Guy Adonadaga, Boateng Ampadu (2026). Impact of Climate Change and Land Use/Land Cover Changes on Sustained Water Flow in The Tamne Catchment of Ghana: A Long-Term Spatio-Temporal Assessment Using The Swat Model. Ecofeminism and Climate Change, 7(1): 17-29.

Table 4(Cont.): Land Conversion and Proportionality Analysis				
2013-2022	GSL	WAT, BBS	8.8	3.33
2013-2022	GSL	AGR	79.2	30.00

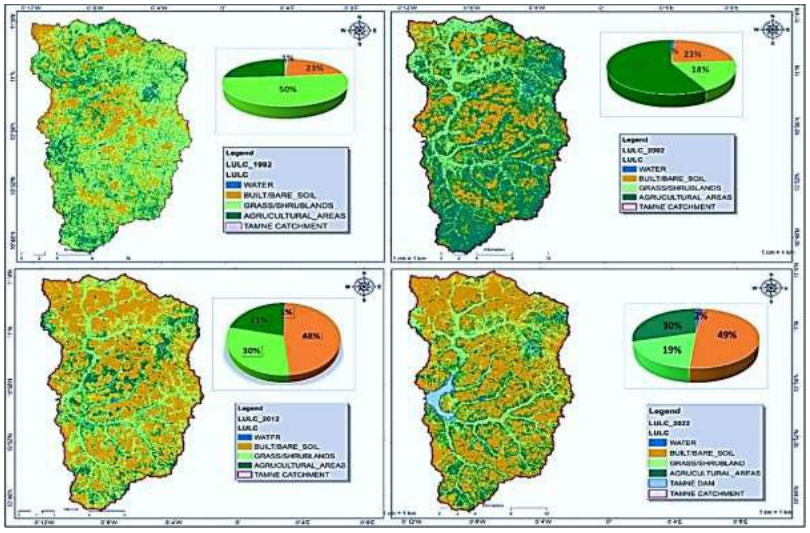

Figure 6: Land use or Land cover change maps and charts for 1992, 2002, 2012 and 2022

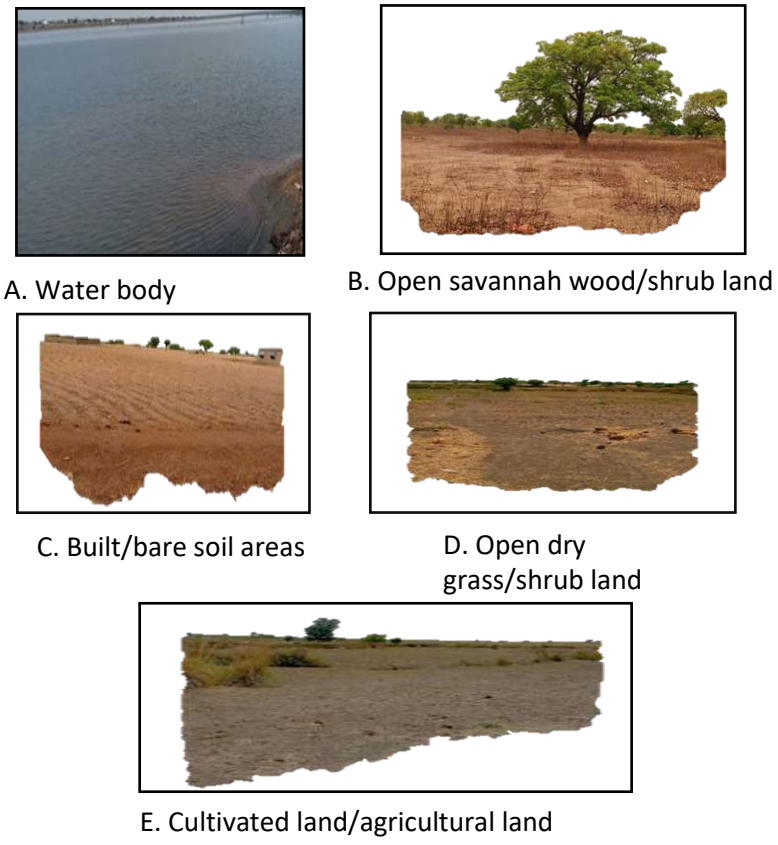

Figure 7: Ground truthing land use/land cover classification in the Tamne catchment

3.2 Trend and Modulation Analysis of Annual Rainfall via the Mann-Kendall Test

Figure 8 illustrates the yearly distribution of rainfall estimated over the Tamne catchment. This demonstrates the overall inter-annual fluctuation of rainfall on an annual basis in the Tamne catchment from 1992 to 2022. The lowest and highest annual rainfall recorded were 521.0 mm and 992.0 mm, respectively, occurring in 2008 and 2012.

Table 5, 6, 7, and 8 display the monthly coefficient of variation (CV) values explaining the phenomenon in statistical terms, while Table 6 shows the Mann-Kendall test statistics for rainfall for the period from 1992 to 2022. Also, the coefficient of variations (CVs) of large values ranging from 101.0% to 950.0% across (Table 5, 6, 7, and 8) consistently for the three decades and cumulatively from 1992 to 2022 indicated monthly rainfall instability, especially between November and April. Small CV values ranging from 75.2% to 188.2% indicated stable monthly rainfall between May and October (CVs) ranged from 13.0% to 87.8% which were scaled from moderate to high variability in intra-seasonal and intra-annual rainfall frequency. The patterns of rainfall in Figure 8 indicate rainfall departure from the mean from 1992 to 2022. Also, the micro- climate pattern is revealed to be completely unpredictable in terms of rainfall and temperature. Rainfall is fluctuating and declining, while temperature is varying and rising. The trend suggested a decreasing and negative trend of rainfall in both monthly and yearly, supported by the Kendall tau (-0.167), S (-2), Sen's slope (-5.124) of rainfall in Table 9, but statistically insignificant with p-value (0.724). Considering Figure 9 below

represented a departure from the mean with negative departures, indicating lower rainfall values than the mean. While positive departures indicate that such annual rainfall values were higher than the mean. Supposedly, the rainfall departures indicate fewer wet seasons (WS) of nine (9) observations in the positive plane, less than the twenty-one (21) observations predicted as dry seasons (DS), over the period with rainfalls below the estimated mean rainfall of 676.77mm in the negative plane, except for 2007, 2019, and 2021, which recorded rainfall nearly at the mean level within the period.

From Table 10 depicted a varying effect of each land usage and land cover type on each hydrological element considered at decadal and inter-decadal scale with 1992 as the base year. Water (WAT) contributes largely to evapotranspiration (ET) with 171mm/H2O in 1992 and increased to 173mm/H2O from 2002 after a decade representing a change of 1.25%. However, it increased again marginally to 173mm/H2O from 2012 representing 0.01% after a decade but decreased from 2022 to 160mm/H2O representing 8.47% respectively. The built/bare soil have impacted ET by 32mm/ H2O in 1992 and increased to 35mm/H2O from 2002, representing an increase of 11.11%. The impact, then lessen to 30mm/H2O and 30mm/H2O from 2012 to 2022 representing 0.17% and 0.07% respectively. Grass/shrub land affected ET by 33mm/H2O in 1992 and increased to 38mm/H2O in 2002 representing 12.06%. But also lessen from 2012 to 2022 to 36mm/H2O and 36mm/H2O representing 5.24% and 0.14% respectively.

Agriculture (AGR) impacted ET by 29mm/H2O in 1992 and changed to 34mm/H2O from 2002 representing an increase of 13.34%, then it again contributed to evapotranspiration (ET) by 36 mm/H2O and 36mm/H2O from 2012 to 2022 an increase representing 4.97% and 0.06% respectively in series. Built/bare soils (BBS) contributed to surface runoff (SQ) as an effect of about 48mm/H2O to 18mm/H2O from 1992 to 2002. It represents 65.83% decrease in 2002. But also affected water yield (WY) by 16mm/H2O and 20mm/H2O from 1992 to 2002 respectively, representing an increase of 18.86% by 2002. But varied from 18mm/H2O in 2002 to 27mm/H2O by 2012 representing 34.21% increase. And 20mm/H2O to 18mm/H2O representing a lower impact of 9.71% on water yield (WY) in 2012. Also, a decrease from 27.04mm/H2O to 17.72mm/H2O representing 52.6% with less impact on surface runoff (SQ) but an increased influenced from 18mm/H2O to 20.02mm/H2O representing 8.9% on water yield in 2022 respectively.

Grass/shrub land impacted surface runoff (SQ) by 10mm/H2O in 1992, 9mm/H2O in 2002 representing 15.91% decrease, then 16.69mm/H2O (44.31%) in 2012 and 22mm/H2O (23.3%) in 2022, with each representing a reduced impact in 2002 and elevated impacts from 2012 to 2022 in time series. Water had zero (0) impact on groundwater in the three decades from 1992 to 2022. But the built/bare soil had zero (0) impact on groundwater (GW) in 1992 but affected groundwater by 14mm/H2O, 20mm/H2O, and 14mm/H2O presenting a decadal variation in 2002, 2012 and 2022 respectively but only indicated an increase of 30.5% from 2002 to 2012. Also, grass/shrub land and agriculture affected groundwater (GW) by 20mm/H2O and 20mm/H2O in 1992 respectively. Grass/shrub land affected groundwater by 22mm/H2O in 2002 and increased to 37mm/H2O in 2012 representing 40.63% but again lessened to 23mm/H2O in 2022. Agriculture contributed to the impact by 22mm/H2O in 2002 but increased to 27mm/H2O in 2012 representing 17.23%. However, it decreased from 27mm/H2O in 2012 to 22mm/H2O by 2022.

Table 5: Decadal monthly rainfall variation from 1992-2001

Month	Min(mm)	Max(mm)	Mean	SD	CV (%)
Jan	0	0.2	0.02	0.06	300.0
Feb	0	1.58	0.24	0.47	195.8
Mar	0	13.6	5.12	5.35	104.5
Apr	0	69.9	11.60	21.83	188.2
May	22.56	108.6	62.78	24.16	38.5
Jun	37.6	66.7	55.16	9.23	16.7
Jul	101.7	252.4	150.0	41.62	27.7
Aug	92.8	300.2	208.88	57.53	27.5
Oct	10.2	99.1	53.64	22.96	42.8
Nov	0	11.03	2.94	3.92	133.3
Dec	0	0.2	0.04	0.07	175.0

Table 6: Decadal monthly rainfall variation from 2002-2011

Month	Min(mm)	Max(mm)	Mean	SD	CV (%)
Jan	0	0.1	0.02	0.13	650.0
Feb	0	0.17	0.03	0.06	200
Mar	0	13.66	5.37	4.30	80.1
Apr	0.07	27.00	4.96	7.93	159.9
May	89.5	181.4	49.9	43.44	87.1
Jun	36.6	89.4	58.43	17.76	30,4
Jul	89.5	181.4	140.27	27.83	19.8
Aug	146..9	320.4	204.51	29.84	14.6

Table 6(Cont.): Decadal monthly rainfall variation from 2002-2011					
Sept	49.4	197.6	134.14	48.09	35.9
Oct	10.0	69.1	48.28	17.95	37.2
Nov	0	0.4	0.07	0.06	85.7
Dec	0	0.2	0.03	0.06	200.0

Table 7: Decadal monthly rainfall variation from 2012-2021					
Month	**Min(mm)**	**Max(mm)**	**Mean**	**SD**	**CV (%)**
Jan	0	0.1	0.01	0.03	300.0
Feb	0	2.14	0.24	0.64	266.7
Mar	0	16.93	3.89	4.96	127.5
Apr	0	26.99	7.53	6.11	81.1
May	0	78.6	28..77	16.11	56.6
Jun	37.2	115.3	65.57	24.03	37.0
Jul	51.3	216.5	147.13	49.61	34.0
Aug	172.6	282.8	238.96	31.86	13.0
Sept	65.2	252	104.19	56.84	55.0
Oct	12.4	251.5	66.12	66.56	101.0
Nov	0	0.4	0.07	0.13	181.0
Dec	0	0.1	0.01	0.095	950.0

Table 8: Cumulative monthly rainfall for the period 1992 – 2022					
Month	**Min(mm)**	**Max(mm)**	**Mean**	**SD**	**CV (%)**
Jan	0	0.2	0.02	0.07	350.0
Feb	0	2.14	0.17	0.46	270.6
Mar	0	16.93	4.70	4.87	103.6
Apr	0	69.90	9.71	16.04	165.2
May	0	164.59	53.1	32.76	61.7
Jun	34.24	115.29	59.75	18.29	30.6
Jul	51.26	252.90	146.69	42.18	28.8
Aug	92.77	320.39	214.96	50.27	23.4
Sept	49.40	252.03	133.08	43.89	33.0
Oct	9.96	251.52	55.80	41.97	75.2
Nov	0	11.03	0.98	2.61	266.3
Dec	0	0.2	0.03	0.06	200.0

Table 9: Mann-Kendall test statistics	
MK-Test parameter	**Measured value**
Kendall´s tau	-0.167
Mann-Kendall test statistic(S)	-2
Var(S)	8
P-value	0.724
Alpha	0.05
Mean	676.867
Standard deviation	119.226

Table 10: Inter-decadal time-scale impact of LULC comparison on selected hydrological components using the SWAT outputs for 1992 to 2022 in mm/H_2O.

Year	**1992**				**2002**				**2012**				**2022**			
Hydrological Components (mm/H2O)	**ET**	**SQ**	**GW**	**WY**	**ET**	**SQ**	**GW**	**WY**	**ET**	**SQ**	**GW**	**WY**	**ET**	**SQ**	**GW**	**WY**
LULC-Class																
WAT	171	0	0	0	173	0	0	0	173	0	0	0	160	0	0	0
BBS	32	48	0	16	36	18	14	20	30	27	20	18	30	18	14	20
GSL	33	10	20	10	38	9	23	19	36	17	38	12	36	22	22	19
AGR	29	21	20	7	34	15	22	19	36	27	27	15	36	7	22	19

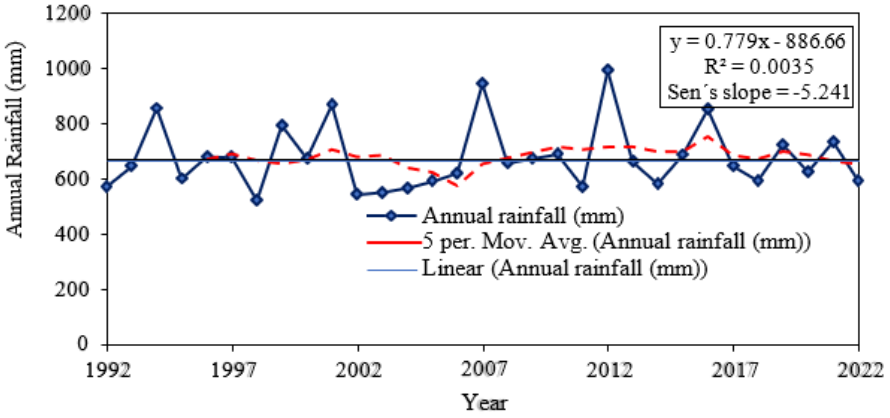

Figure 8: Trend of Average Annual Rainfall for Tamne catchment for 1992-2022

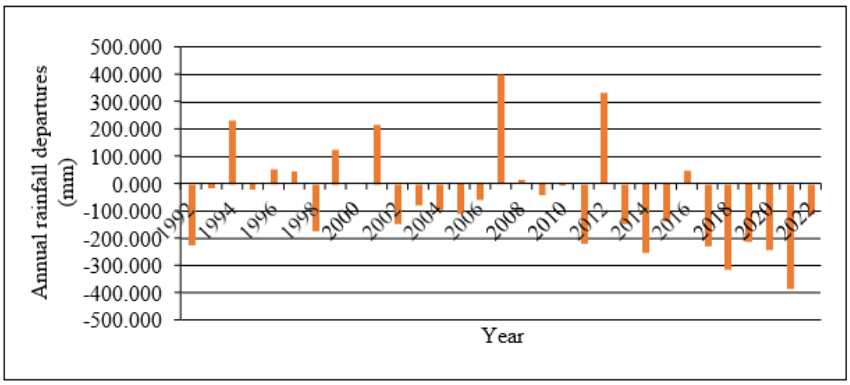

Figure 9: Rainfall departure from the mean chart from 1992-2022

3.3 Monthly Trend and Distribution of Mean Precipitation, Minimum Temperature, and Maximum Temperature from 1992-2021

Figure 10 shows the trend and distribution of monthly mean rainfall, minimum temperature, and maximum temperature from 1992 to 2022, indicating unstable atmospheric conditions resulting in fluctuating monthly average minimum and maximum temperatures observed by the model. The inter-decadal monthly means of the averages of the minimum and maximum temperatures for the three decades are 21.80°C and 37.93°C, respectively, and the inter-annual monthly mean rainfall is estimated as 56.26 mm for the three decades. The summary is provided as follows:

The average minimum temperature was predicted to be 21.39°C in 1992 as the baseline. In reference, it has been on an increasing trajectory.

Sequentially, it rose to 21.61°C (2001), 21.89°C (2011), and 22.31°C (2021). Over the three decades, the predicted variance stood at 0.92°C. Average maximum temperatures were 37.53°C in 1992 as the base year. It saw a rise to 38.13°C (2001), 37.90°C (2011), and 38.15°C (2021), indicating an average rise of 0.62°C for the period.

Monthly rainfall showed variations with 47.66mm (1992), 45.23mm (2001), 82.67mm (2011), and 49.47mm (2021) Going by this, the first decade shown a drop by 2.43mm between 1992 and 2001, while there was an increase from 2002 to 2011 of 37.44mm but again declined by 33.2mm between 2012 and 2021.The difference in the decadal average in maximum temperature was 0°C (1992), 0.6°C (2001), -0.23°C (2011), and 0.25°C (2021), with a decrease of -0.23°C in the period between 2002 and 2011, as shown in Table 11.

Table 11: Decadal means of rainfall, minimum and maximum temperatures between 1992 and 2022.

Year	Average monthly rainfall (mm)	Minimum temperature (°C)	Maximum temperature (°C)	Average temperature (°C)	Difference in max temp.(°C)
1992	47.66	29.46	37.53	21.39	0.00
1992-2001	45.23	29.87	38.13	21.61	0.60
2002-2011	82.67	29.90	37.90	21.89	-0.23
2012-2021	49.47	30.23	38.15	22.31	0.25

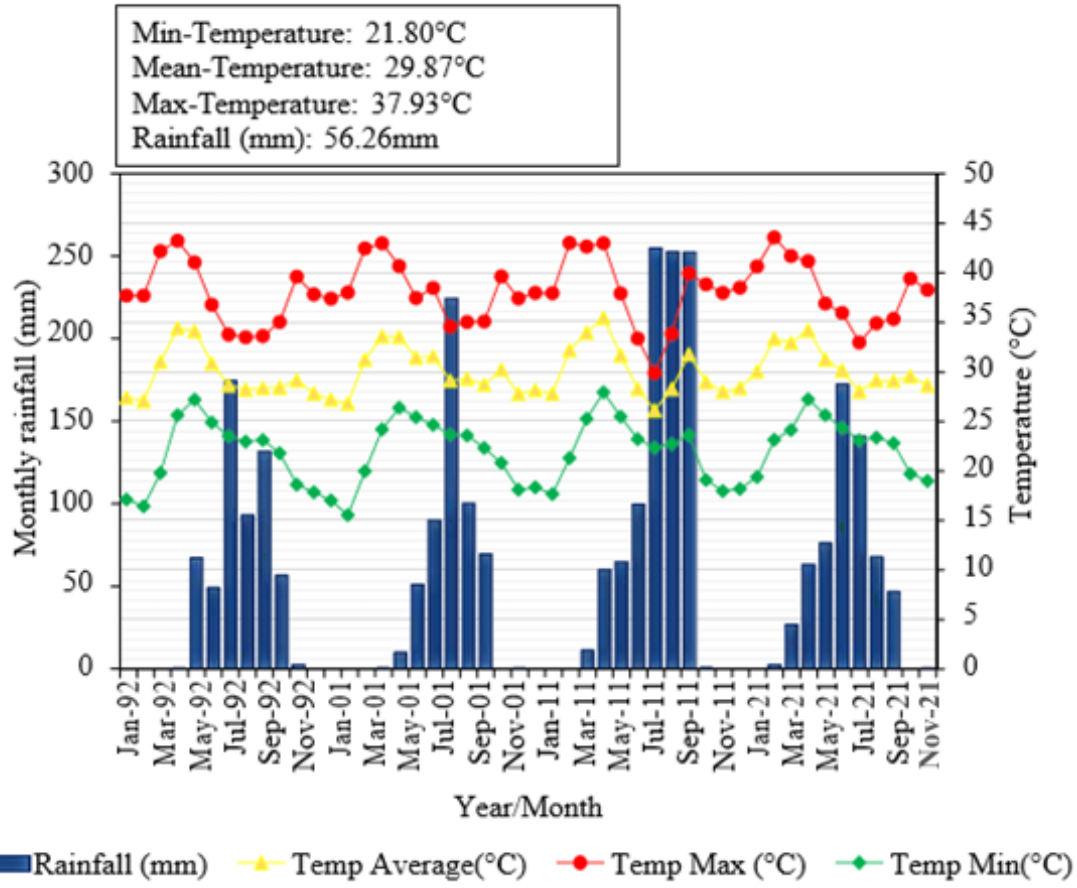

Figure 10: Monthly rainfall, minimum and maximum temperature from 1992 to 2022

3.4 SWAT Model Hydrologic calibration-validation

A plot of the observed and simulated flows in the Tamne Catchment is shown in Figure 11. Figure 11 shows that simulated flows follow the observed flows pattern and predicted peak flows as well. Figure 11 also shows that the model over and under predicted the observed flows consistently during the recession periods. The model performance for both calibration and validation has been presented in Table 12.

Table 12: Different Objective Functions used in the SUFI-2 Calibration process of the SWAT- CUP on Water Balance Analysis (WBA).

Objective function	Definition of function	Calibration	Validation
P-factor	Percentage of measured data bracketed by 95%	0.75	0.35
R-factor	The average thickness of the 95PPU envelope.	0.78	0.28
R^2	Coefficient of Determination	0.71	0.71

Table 12(Count): Different Objective Functions used in the SUFI-2 Calibration process of the SWAT- CUP on Water Balance Analysis (WBA).			
NSE	Nash-Sutcliffe Efficiency	0.71	0.71
KGE	Kling-Gupta Efficiency	0.74	0.74
PBIAS	Percent Bias	13.8	13.8
bR^2	Modified coefficient of	0.51	0.51
RSR	determination Root mean square error	0.54	0.54
MNS	Modified Nash-Sutcliffe	0.55	0.00

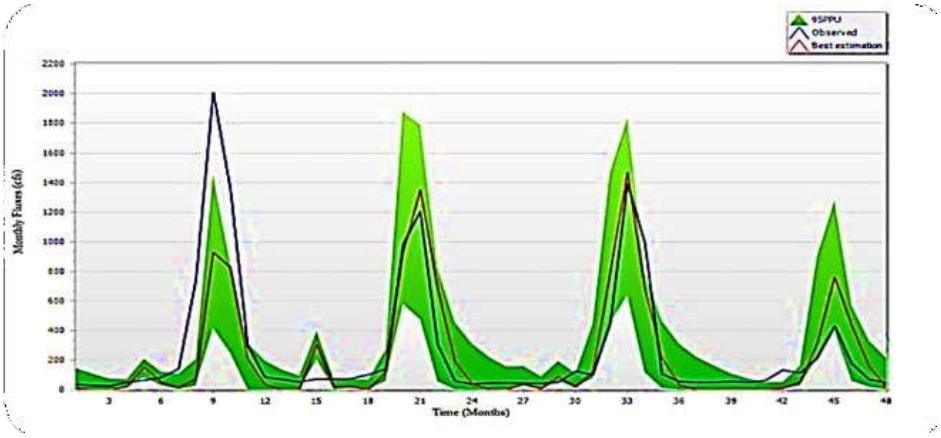

Figure 11: Model output of SWAT-CUP against observed flows with 95% prediction uncertainty

3.5 Statistics of Calibration and Validation

Table 13 shows the P-values for the sensitivity parameters. Considering the P-values, relatively shallow aquifer storage factor (r_SA_ST –hru) and the shallow aquifer storage returning to the root zone for Revap (r_REVAP-gw) initially with a p-value of approximately zero (0) are the first and second most sensitive criteria, indicating that irrigation dams and land use control the inflow. Parameters such as the threshold depth of water as deep aquifer recharge f (r_RCHRG_DA-gw) through to surface runoff generated (r_SURFQ-GEN-hru) with p-values of 0.80 to 0.96, respectively, were also found to be extremely vulnerable. These parameters relate to groundwater decline and alteration in supplied precipitation affecting refill analogous to the inferences from the study report.

Table 13: Statistics of the p-value for the sensitivity of parameters			
Parameter	Parameter definition	*P-value*	Ranking
r_SA_ST-hru	Shallow aquifer storage	0.00	1
r_REVAP-gw	Water in shallow aquifers returning	0.00	2
r_LATQ-hru	Lateral flow	0.40	3
r_RCHRG_DA-gw	Deep aquifer recharge	0.80	4
r_GWQMN-gw	Groundwater recharge	0.80	5
r_SW-INIT-hru	Soil water content for the period	0.82	6
r_SW_END-hru	Soil water content at the end of the period	0.84	7
r_DAILY_CN-hru	Average curve number for the period	0.87	8
r_PERC-hru	Percolation	0.92	9
r_DA_ST-gw	Deep aquifer storage	0.94	10
r_SURFQ-GEN-hru	Surface runoff generated	0.96	11

5. Conclusion and Recommendation

Land use/land cover changes driven primarily by human activities have significantly altered the hydrological dynamics of the Tamne catchment. These changes led to an increase in surface runoff and evapotranspiration. The results showed a decrease in shallow aquifer recharge and groundwater discharge. These trends were consistent across 236 Hydrologic Response Units (HRUs) and 27 sub-catchments, indicating widespread fluctuations in hydrological components due to LULC change.

Rainfall exhibited a decreasing and negative trend in both monthly and annual analysis. Rainfall variability was evident, but not statistically significant. Concurrently, temperatures increased highlighting a warming trend.

The sensitivity analysis using the SWAT model identified shallow aquifer storage factor and REVAP return flow to the root zone as highly sensitive parameters. Deep aquifer recharge and surface runoff generation were extremely vulnerable components.

Declining rainfall and rising temperatures are insignificantly influencing water availability in the Tamne catchment. The findings emphasize the need for sustainable land use planning and water resource management to ensure long-term agricultural productivity and natural resource conservation in the region.

ACKNOWLEDGMENT

I greatly appreciate you Lord, for you have highly favored me in life. My immense appreciation goes to my sweet wife Mrs. Awini Cynthia Alaadi for her invaluable support. Also, Mr. Mbilla Moses and Alhaji Ayass Awelisah, please accept my appreciation for the encouragement in the realization of this research work.

REFERENCES

Abbam, T., Amoako, F. J., Dash, J., and Padmadas, S. S., 2018. Spatio-temporal variations in rainfall and temperature in Ghana over the twentieth century, 1900–2014. Earth and Space Science, 5(4), Pp. 120–132. https://doi.org/10.1002/2017EA000327

Abbas, M., Zhao, L., and Wang, Y., 2022. Perspective impact on water environment and hydrological regime owing to climate change: A review. Hydrology, 9(11), 203. https://www.mdpi.com/2306-5338/9/11/203

Abbaspour, K. C., 2015. SWAT-Calibration and Uncertainty Programs: A User Manual. SWAT, Pp. 17–66. https://swat.tamu.edu

Abdi, H., 2010. Coefficient of variation. Encyclopedia of Research Design, 1(5), Pp. 169–171. https://www.utdallas.edu/~herve/abdi-cv2010-pretty.pdf

Abungba, J. A., Adjei, K. A., Gyamfi, C., Odai, S. N., Pingale, S. M., and Khare, D., 2022. Implications of land use/land cover changes on Black Volta basin future water resources in Ghana. Sustainability, 14(19), 12383. https://doi.org/10.3390/SU141912383

Ait M'Barek, S., Bouslihim, Y., Rochdi, A., and Miftah, A., 2023. Effect of LULC data resolution on hydrological and erosion modeling using SWAT model. Modeling Earth Systems and Environment, 9(1), Pp. 831–846. https://doi.org/10.1007/s40808-022-01537-w

Ampadu, B., 2021. Overview of hydrological and climatic studies in Africa: The case of Ghana. Cogent Engineering, 8(1), 1914288.

Ampadu, B., Sackey, I., and Cudjoe, E., 2019. Rainfall distribution in the Upper East Region of Ghana. Ghana Journal of Science, 6(2), Pp. 45–59. https://doi.org/10.47881/168.967x

Ampofo, S., Annor, T., Aryee, J. N. A., Atiah, W. A., and Amekudzi, L. K., 2023. Long-term spatio-temporal variability and change in rainfall over Ghana (1960–2015). Scientific Africa, 19. https://doi.org/10.1016/j.sciaf-2023-e01588

Ampofo, S., Gyekye, E., and Ampadu, B., 2021. Modelling soil and water dynamics in Black Volta Basin using the Soil and Water Assessment Tool (SWAT). Ghana Journal of Science, Technology and Development, 7(2). https://doi.org/10.47881/259.967x

Ampofo, S., Manu, M. A. B., and Ampadu, B., 2022. Impact of land use and land cover changes on hydrological components of the Oti Sub-Basin of Ghana. Ghana Journal of Science, 8(2), Pp. 66–70. https://doi.org/10.47881/259.967x

Arnold, J. G., Moriasi, D. N., Gassman, P. W., Abbaspour, K. C., White, M. J., Srinivasan, R., and Jha, M. K., 2012. SWAT: Model use, calibration, and validation. Transactions of the ASABE, 55(4), Pp. 1491–1508. https://elibrary.asabe.org/abstract.asp?aid=42256

Asamoah, Y., and Ansah-Mensah, K., 2020. Temporal description of annual temperature and rainfall in the Bawku Area of Ghana. Advances in Meteorology, 2020, Article ID 34021781, Pp. 1–18. https://doi.org/10.1155/2020/3402178

Asante, F. A., and Amuakwa-Mensah, F., 2014. Climate change and variability in Ghana: Stocktaking. Climate, 3(1), Pp. 78–101. https://www.mdpi.com/2225-1154/3/1/78

Asserup, P., and Eklöf, M., 2000. Estimation of the soil moisture distribution in the Tamne River Basin, Upper East Region, Ghana. Lunds universitets Naturgeografiska Institution – Seminarieuppsatser. https://lup.lub.lu.se/student-papers/search/publication/1332898

Awotwi, A., Annor, T., and Anornu, G. K., 2021. Climate change impacts on streamflow in a tropical basin of Ghana, West Africa. Journal of Hydrology: Regional Studies, 34, 100805. https://doi.org/10.1016/j.erh.2021.100805

Awotwi, A., Anornu, G. K., Quaye-Ballard, A. J., Annor, T., Forkuo, E. K., Harris, E., Agyekum, J., and Terlabie, L. J., 2019. Water balance responses to land-use/land-cover changes in the Pra River Basin of Ghana, 1986–2025. Catena, 182, 104129. https://doi.org/10.1016/j.catena.2019.104129

Baker, T. J., and Miller, S. N., 2013. Using the Soil and Water Assessment Tool (SWAT) to assess land use impact on water resources in an East African watershed. Journal of Hydrology, 486, Pp. 100–111. https://www.sciencedirect.com/science/article/pii/S002216941300098X

Bessah, E., Raji, O. A., Taiwo, O. J., Agodzo, K. S., Ololade, O. O., and Strapasson, A., 2020. Hydrological responses to climate and land use changes: The paradox of regional and local climate effect in the Pra River Basin of Ghana. Journal of Hydrology: Regional Studies, 27, 100654. https://doi.org/10.1016/j.ejrh.2019.100654

Brown, C. E., 1998. Coefficient of variation. In Applied Multivariate Statistics in Geohydrology and Related Sciences (Pp. 155–157). https://doi.org/10.1007/978-642-80328-4

Clark, M. P., Wilby, R. L., Gutmann, E. D., Vano, J. A., Gangopadhyay, S., Wood, A. W., and Brekke, L. D., 2016. Characterizing uncertainty of the hydrologic impacts of climate change. Current Climate Change Reports, 2(2), Pp. 55–64. https://doi.org/10.1007/s40641-016-0034-x

Copernicus, 2023. 2023 is the hottest year on record, with global temperatures close to the 1.5°C limit. Retrieved from https://climate.copernicus.eu

Da Silva, R. M., Santos, C. A., Moreira, M., Corte-Real, J., Silva, V. C., and Medeiros, I. C., 2015. Rainfall and river flow trends using Mann–Kendall and Sen's slope estimator statistical tests in the Cobres River Basin. Natural Hazards, 77(2), Pp. 1205–1221. https://doi.org/10.1007/s11069-015-1644-7

Dankwa, P., Cudjoe, E., Amuah, E. E. Y., Kazapoe, R. W., and Agyemang, E. P., 2021. Analyzing and forecasting rainfall patterns in the Manga-Bawku area, northeastern Ghana: Possible implication of climate change. Environmental Challenges, 5, 100354. https://doi.org/10.1016/j.envc.2021.100354

Dile, Y. T., Daggupati, P., George, C., Srinivasan, R., and Arnold, J., 2016. Introducing a new open-source GIS user interface for the SWAT model. Environmental Modelling and Software, 85, Pp. 129–138. https://doi.org/10.1016/j.envsoft.2016.09.004

Efthimiou, N., 2018. Hydrological simulation using the SWAT model: The case of Kalamas River catchment. Journal of Applied Water Engineering and Research, 6(3), Pp. 210–227. https://doi.org/10.1080/23249676.2016.1265471

Gassman, P. W., Sadeghi, A. M., and Srinivasan, R., 2014. Applications of the SWAT model special section: Overview and insights. Journal of Environmental Quality, 43(1), Pp. 1–8. https://doi.org/10.2134/jeq2013.11.0466

Gbangou, T., Ludwig, F., Slobbe, E. V., Gruell, W., and Kranjac-Berisavlevic, G., 2020. Rainfall and dry spells occurrence in Ghana: Trends and seasonal predictions with a dynamical and statistical model. Theoretical and Applied Climatology, 141, Pp. 371–387. https://doi.org/10.1007/s00704-020-03212-5

Ghana Irrigation Development Authority, 2021. E-Agriculture Portal. Retrieved from http://www.gida.gov.gh / http://www.e.agriculture.gov.gh (e.agriculture.gov.gh in Bing)

Ghana Statistical Service, 2021. 2021 Population and Housing Census, General Report Volume 3A: Population of Regions and Districts. November 2021. Retrieved from www.statsghana.gov.gh

Gordon, C., Nukpezah, D., Tweneboah-Lawson, E., Ofori, B. D., Yirenga-Tawiah, D., Pabi, O., Ayivor, J. S., Koranteng, S., Darko, D., and Mensah, A. M., 2013. West Africa – Water resources vulnerability using a multidimensional approach: Case study of Volta Basin. In Climate Vulnerability: Understanding and Addressing Threats to Water Resources (Pp. 283–309). https://doi.org/10.1016/B978-0-12-384703-4.00518-9

Guug, S. S., Shaibu, A. G., and Kasei, A. R., 2020. Application of SWAT hydrological model for assessing water availability at the Sherigu

catchment of Ghana and Southern Burkina Faso. Hydro-Research, 3, Pp. 124–133. https://doi.org/10.1016/j.hydres.2020.10-002

IPCC, 2022. AR6 WGII Chapter 2, 4, 8 and 9: Impacts, Adaptation and Vulnerability. Intergovernmental Panel on Climate Change.

Issahaku, A. R., 2023. Impacts of climate change, land use and land cover changes on watersheds in the Upper East Region of Ghana. Journal of Geography, Environment and Earth Science International, 27(3), Pp. 33–44.

Issahaku, A. R., Campion, B. B., and Edziyie, R., 2016. Rainfall and temperature changes and variability in the Upper East Region of Ghana. Earth and Space Science, 3(8), Pp. 284–294. https://doi.org/10.1002/2016EA000161

Kasei, R. A., Ampadu, B., and Yalevu, S., 2014. Impacts of climate variability on food security in Northern Ghana. Journal of Earth Sciences and Geotechnical Engineering, 4(3), Pp. 47–59.

Khalid, C., 2018. Hydrological modeling of the Mikkés watershed (Morocco) using ArcSWAT model. Sustainable Water Resources Management, 4(1), Pp. 105–115. https://doi.org/10.1007/s40899-017-0145-0

Klutse, N. A. B., Owusu, A., and Boafo, Y. A., 2020. Projected temperature increases over northern Ghana. SN Applied Sciences, 2, Pp. 1–14. https://doi.org/10.1007/s42452-020

Kpoti, K., Antwi, O. E., and Kabo-bah, A. T., 2016. Impacts of rainfall variability, land use and land cover change on stream flow of the Black Volta Basin, West Africa. Hydrology, 3(3), 26. https://doi.org/10.3390/hydrology3030026

Lovie, P., 2005. Coefficient of variation. In Encyclopedia of Statistics in Behavioral Science. https://doi.org/10.1002/0470013192.659107

Maru, H., Hailesiassie, A., and Zeleke, T., 2023. Analysis of land use/land cover change on streamflow and surface water availability in Awash Basin, Ethiopia. Geomatics, Natural Hazards and Risk, 14(1), Pp. 1–25. https://doi.org/10.1080/19475705.2022.2163193

Ministry of Food and Agriculture, 2022. Annual Report. Retrieved from http://mofa.gov.gh.directorates (mofa.gov.gh.directorates in Bing)

Mishio, M., 2021. Improved management of the water and energy resources in the Volta Basin (Master's thesis, NTNU). Retrieved from https://ntnuopen.ntnu.no/ntnu-xmlui/handle/11250/2824233 (ntnuopen.ntnu.no in Bing)

Mishra, R. K., 2023. Fresh water availability and its global challenge. British Journal of Multidisciplinary and Advanced Studies, 4(3), Pp. 1–78. https://doi.org/10.37745/bjmas2022.0208

Nasta, P., Allocca, C., and Deidda, R., 2020. Assessing the impact of seasonal rainfall anomalies on catchment-scale water balance components. Hydrology and Earth System Sciences, 24(6), Pp. 3211–3227. https://doi.org/10.5194/hess-24-3211-2020

Ndehedehe, C. E., Awange, J. L., Agutu, N. O., and Okwuashi, O., 2018. Changes in hydro-meteorological conditions over tropical West Africa (1980–2015) and links to global climate. Global and Planetary Change, 162, Pp. 321–341. https://doi.org/10.1016/j.gloplacha.2017.11.006

Obuobie, E., Kankam-Yeboah, K., and Amisigo, B., 2012. Assessment of vulnerability of river basins in Ghana to water stress conditions under climate change. Journal of Water and Climate Change, 3(4), Pp. 276–286. https://doi.org/10.2166/wcc.2012.030

Okofo, L. B., and Martienssen, M., 2022. A three-dimensional numerical groundwater flow model to assess the feasibility of managed aquifer recharge in the Tamne River Basin of Ghana. Hydrogeology Journal, 30(4), Pp. 1071–1087. https://doi.org/10.1007/s10040-022-02492-7

Okofo, L. B., Bedu-Addo, K., and Martienssen, M., 2022. Characterization of groundwater in the Tamnean Plutonic Suite aquifers using hydrogeochemical and multivariate statistical evidence: A study in the Garu-Tempane District, Upper East Region of Ghana. Applied Water Science, 12(2), 22. https://doi.org/10.1007/s12665-021-10081-2

Osei, M. A., Amekudzi, L. K., Wemegah, D. D., Preko, K., Gyawu, E. S., and Obiri-Danso, K., 2019. The impact of climate and land-use changes on the hydrological processes of Owabi catchment from SWAT analysis. Journal of Hydrology: Regional Studies, 25, 100620. https://doi.org/10.1016/j.ejrh.2019.100620

Pandi, D., Kothandaraman, S., and Kuppusamy, M., 2023. Simulation of water balance components using SWAT model at sub-catchment level. Sustainability, 15(2), 1438. https://doi.org/10.3390/su15021438

Quaye-Ballard, J. A., Okrah, T. M., Andam-Akorful, S. A., et al., 2020. Spatiotemporal dynamics of rainfall in Upper East Region of Ghana, West Africa, 1981–2016. SN Applied Sciences, 2, Pp. 1–12. https://doi.org/10.1007/s42452-020-03463-x

Sanogo, A., Kabange, R. S., Owusu, P. A., Djire, B. I., Dorko, R. F., and Dia, N., 2023. Investigation into recent temperature and rainfall trends in Mali using Mann-Kendall trend test: Case study of Bamako. Journal of Geoscience and Environment Protection, 11(3), Pp. 155–172. https://doi.org/10.4236/gep.2023.113011

Talib, M. N. A., Ahmed, M., Naseer, M. M., Slusarczyk, B., and Popp, J., 2021. The long-run impacts of temperature and rainfall on agricultural growth in Sub-Saharan Africa. Sustainability, 13(2), 595. https://doi.org/10.3390/su130595

Taylor, R. G., Scanlon, B., Döll, P., Rodell, M., Van Beek, R., Wada, Y., and Treidel, H., 2013. Groundwater and climate change. Nature Climate Change, 3(4), Pp. 322–329. https://doi.org/10.1038/nclimate1744

Trenberth, K. E., 2011. Changes in precipitation with climate change. Climate Research, 47(1–2), Pp. 123–138. https://doi.org/10.3354/cr00953

United Nations, 2006. World Water Development Report. Retrieved from http://www.unwater.org

Wang, F., Shap, W., Yu, H., Ken, G., He, X., and Zhang, D., 2020. Re-evaluation of the power of the Mann-Kendall test for detecting monotonic trends in hydrometeorological time series. Frontiers in Earth Science, 8, Article 14, Pp. 1–12. https://doi.org/10.3389/feart.2020.00014

Xiang, X., Ao, T., Xiao, Q., Li, X., Zghou, L., Bi, Y., and Guo, J., 2022. Parameter sensitivity analysis of SWAT modeling in the Upper Heihe River Basin using four typical approaches. Applied Sciences, 12(19), 9862. https://doi.org/10.3390/app12199862